Journal of Inflammation Research

Dovepress
Taylor & Francis Group

Open Access Full Text Article

ORIGINAL RESEARCH

Immune Microenvironmental Differences Between Obese and Healthy People in a High-Altitude Hypoxic Environment

Xiaoyan Pu[1,*], Yaxuan Wang[1,*], Xue Lin[2], Jun Zhao[1], Chongyang Dai[1], Yonggui Ma[3], Peijun Shi[3–5]

[1]Medical College, Qinghai University, Xining, Qinghai Province, 810016, People's Republic of China; [2]Department of Pulmonary and Critical Care Medicine, West China Hospital, Sichuan University, Chengdu, Sichuan Province, 610000, People's Republic of China; [3]College of Life Sciences, Qinghai Normal University, Xining, Qinghai Province, 810016, People's Republic of China; [4]State Key Laboratory of Earth Surface Processes and Resource Ecology, Beijing Normal University, Beijing, 100875, People's Republic of China; [5]Faculty of Geographical Science, Beijing Normal University, Beijing, 100875, People's Republic of China

*These authors contributed equally to this work

Correspondence: Peijun Shi, State Key Laboratory of Earth Surface Processes and Resource Ecology, Beijing Normal University, Beijing, 100875, People's Republic of China, Tel +86 10 58808179, Email spj@bnu.edu.cn; Yonggui Ma, College of Life Sciences, Qinghai Normal University, Xining, Qinghai Province, 810016, People's Republic of China, Tel +86 18697243977, Email 1261602778@qq.com

Purpose: Rapid ascent to high altitudes can induce altitude illness, with obesity potentially exacerbating the hypoxic response. This study aimed to preliminarily explore the pathogenesis by comparing the immune microenvironment in obese versus normal-weight organisms after acute hypoxic exposure, and to identify potential biomarkers.

Methods: Single-cell RNA sequencing was performed to profile the immune landscape following acute hypoxic injury. Animal experiments were conducted to validate key findings.

Results: Single-cell analysis revealed a reduced proportion of Treg cells in obese subjects under hypoxia, suggesting a link to disease severity. This was corroborated in animal models, where obese, hypoxic rats (severely injured group) exhibited significantly fewer Treg cells compared to normal-weight, hypoxic rats (mildly injured group). Analysis of key transcription factors, including FOXP3, HIF-1α, IFN-γ, and TNF-α, showed expression trends consistent with the single-cell data.

Conclusion: Our exploratory research indicates that obesity-associated impairment of Treg cell abundance and function may underlie severe hypoxic injury at high altitude. Treg cells represent a promising biomarker for risk assessment and early intervention in altitude illness.

Keywords: hypoxia, single-cell sequencing, obesity, Treg cells, biomarker

Introduction

The high-altitude hypoxic environment continues to pose significant challenges to human health, with profound impacts on multiple physiological systems including cardiovascular, respiratory, and metabolic functions.[1–4] Emerging evidence has revealed that hypoxia-induced inflammatory responses and subsequent immune microenvironment dysregulation represent crucial aspects of physiological adaptation to high-altitude conditions.[5–8] Particularly, regulatory T cells (Tregs), which play a pivotal role in maintaining immune homeostasis, have garnered substantial attention regarding their dynamic alterations under hypoxic stress.[9] Research demonstrates that hypoxia-inducible factor HIF-1α can directly regulate FOXP3 expression and functional stability in Tregs, suggesting Tregs may serve as a critical bridge connecting hypoxia and immune adaptation.[10]

Concurrently, the global prevalence of obesity has increased dramatically, with obesity itself being recognized as a chronic low-grade inflammatory state.[11] This condition is characterized by significant immune system disturbances, wherein Treg dysfunction in adipose tissue has been established as a key driver of obesity-associated metabolic

Received: 27 August 2025
Accepted: 23 October 2025
Published: 11 November 2025

inflammation.[12,13] When obese individuals encounter high-altitude hypoxic environments, pre-existing immunometabolic disturbances may interact with novel hypoxic stressors, potentially exacerbating pathological responses.[14] It has been hypothesized that the heightened susceptibility of obese individuals to high-altitude illnesses may be associated with further impairment of Treg function, leading to disruption of the delicate balance between immunosuppression and inflammation.[15]

Immune cell functionality and response patterns in obese populations may substantially differ from those in healthy individuals, potentially influencing their adaptive capacity and coping strategies under high-altitude hypoxia.[16,17] However, the precise alterations in the peripheral immune microenvironment, particularly in Treg subsets, among obese individuals during acute high-altitude exposure remain inadequately characterized.

Therefore, this study aims to comprehensively investigate the physiological and immunological differences in the immune microenvironment, with special emphasis on Treg cells, between obese and normal-weight individuals under high-altitude hypoxic conditions. By integrating clinical manifestations, physiological parameters, and peripheral blood single-cell sequencing data, we focus on analyzing the composition, functional status, and hypoxic stress responses of Tregs and other immune cell subsets. Our objective is to identify novel immunological biomarkers associated with high-altitude illness severity, thereby providing scientific evidence for early diagnosis and risk intervention strategies.

Materials and Methods

Establishment of the Obese Animal Model and Hypoxic Stimulation

Sample Collection and Processing

Twelve 6-week-old SPF grade male SD rats (purchased from the Laboratory Animal Center of Beijing Weitong Lihua Experimental Animal Technology Co.) with an initial weight of 180 ~ 200 g. Using a Table of Random Numbers, rats were randomly divided into Control group (n=6) and Obesity group (n=6). The rats in the Obesity group were given 60% fat-fed high-fat diet (HFD, Rodent diet with 60 kcal% fat, D12492; Research diets, New Brunswick, New Jersey, USA),[18] and the rats in the Normal group were given normal maintenance diet (NC, growth and reproduction diet, SPFSLFZ003, SPF Biotechnology, Beijing, China). They were kept in an environment with a temperature of 22 ± 2°C, humidity of 40 ~ 70%, and a 12-h light-dark cycle. The rats were kept for a total of 8 weeks, and their body weight was monitored and Lee's index was calculated every 2 weeks. After successfully constructing the obese rat model, the two groups of rats were subjected to hypoxic stress in a hypobaric chamber (AVIC, Fenglei, Low pressure Oxygen Cabin) at a simulated altitude of 6000 m for 72 h.[19] At the end of this period, the rats were anesthetized to measure the partial pressure of oxygen and oxygen saturation. Following these measurements, euthanasia was performed via intraperitoneal injection of an overdose of sodium pentobarbital. Subsequently, whole blood samples, serum obtained after blood centrifugation, and lung tissues were collected for subsequent experimental analyses. (For all animal experiments, the sample size per group was set at $n \geq 6$, based on established empirical laboratory practice).

Arterial Blood Gas Analysis

After anesthetizing the rats by intraperitoneal injection of sodium pentobarbital (MERCK, Beijing Zhijie Fangyuan Technology Co., LTD) at a dose of 45 mg/kg, the abdominal skin of the rats was incised, and 1 mL of whole blood was withdrawn from the abdominal aorta using a blood gas needle, and the arterial blood samples were analyzed immediately by measurement using a fully automated blood gas analyzer (Sysmex Japan). Parameters evaluated included dynamic PaO_2 and SaO_2. The remaining whole blood was withdrawn for centrifugation and serum was collected for post-academic experiments.

Hematoxylin and Eosin (H&E) Staining to Observe the Histopathological Changes of the Lung

After the rats were executed, tissues from the lower lobe of the right lung, measuring 5 mm×5 mm×5 mm, were taken, rinsed, and fixed in 4% paraformaldehyde solution (BL539A, a product of TaKaRa, Japan). After routine paraffin embedding, 5 μm thick paraffin sections were made and stained with H&E staining kit (G1120, TaKaRa, Japan), and the morphological and structural changes of the rat lung tissues in each group were observed with an optical microscope (Model CX-2 1, Olympus, Japan) after magnification of 400 times.

Biochemical Analyzer for the Determination of Four Lipid Levels in Rats

Total cholesterol (TC), triglycerides (TG), low-density lipoprotein (LDL), high-density lipoprotein (HDL) and very-low-density lipoprotein (VLDL) were measured in plasma using a Hitachi 7020 fully automated biochemical analyzer (Hitachi High-tech Co., Ltd., Japan).

ELISA for Serum Leptin and Lipocalin Levels in Rats

Using ELISA kits to measure the concentrations of adiponectin and leptin in serum according to the instructions (Stock numbers HB057-Ra, HB349-Ra, respectively; IHengyuan Biotechnology Co., LTD, Shanghai, China).

Volunteer Recruitment and Clinical Data Collection

Volunteer Recruitment

Volunteers were recruited from Qinghai Provincial People's Hospital and Qinghai University between April and June 2022. Inclusion criteria: (1) first-time travel or work in high-altitude areas; (2) From different plain areas or low altitude provinces (altitude 0–1500 m); (3) Age under 45 years old, gender not limited. Exclusion criteria: (1) History of organic cardiovascular disease, significant arrhythmia, or resting heart rate >100 beats/min; stage 2 hypertension or higher; (2) Chronic respiratory diseases or moderate-to-severe obstructive pulmonary disease; (3) Diabetes mellitus with poor glycemic control; (4) Active upper respiratory infection, acute tracheobronchitis, or pneumonia meeting either criterion: a) Body temperature ≥38°C, b) Temperature <38°C with significant symptoms (cough, sputum production, or chest tightness); (5) Prior occurrence at moderate altitude (1,500–3,000 m) of altitude-related symptoms (headache, dizziness, chest tightness); (6) Pregnancy beyond first trimester (>12 gestational weeks); (7) Suffering from blood diseases such as anemia and polycythemia; (8) Being in menopause, with obvious symptoms such as chest tightness and shortness of breath, and excluding organic diseases; (9) Patients with hysteria, epilepsy, and mental illness; (10) Not cooperating with this researcher.

Eight healthy adult male volunteers were recruited, and according to body mass index (BMI), the volunteers were divided into overweight group (BMI ≥ 24, n=4) and normal weight group (18< BMI < 24, n=4), and the two groups of volunteers travelled to the plateau (Mado County, Qinghai Province, China, 4200 m) together (The average annual oxygen content in Mado County is 154.66g/m^3). Before going to the plateau, on the first, third and fifth days of entering the plateau, we recorded the Louis Lake scores of the above volunteers, and detected the clinical symptoms, blood gas indexes, blood routine indexes, blood biochemistry, urine routine, inflammatory factors and other indexes, and at the same time, we took peripheral blood of the patients on the first, third and fifth days of entering the plateau to carry out the subsequent experimental analyses (For human volunteers, the sample size was subject to the availability of human specimens and ethical approval, and was ultimately determined to be eight healthy males).

Collection of Clinical Indicators Related to Plateau Reaction

Lake Louise Score (LLS) and Peripheral Oxygen Saturation

LLS self-assessment form was distributed to volunteers of both groups after entering the high-altitude and low-oxygen area, and the self-reported scores were classified as mild (3–5), moderate (6–9) or severe (10–12) in LLS.[20] LLS of 3 or more and accompanied by headache symptoms can be clinically diagnosed as Altitude Mountain Sickness (AMS), and LLS of less than 3 indicates that AMS is not present. Physical examination was performed at the local hospital to check the oxygen saturation of the peripheral blood of the patients.

Detection of Clinical Indicators

Peripheral blood and mid-stream urine samples were collected from volunteers. To ensure analytical accuracy, all samples were processed immediately after collection. For complete blood count analysis, peripheral blood was collected in EDTA-anticoagulated tubes and stored at 4°C, with testing completed within 2 hours. For serum 25-(OH)D detection, blood was collected in clot activator tubes, followed by centrifugation for serum separation, and the serum was stored at 4°C. Urine samples were stored at 4°C and tested within 1 hour after collection. Repeated freeze-thaw cycles were avoided for all samples. Blood routine analysis was performed using an automated hematology analyzer (XN-9000, Sysmex, Japan). The measured parameters included white blood cell count, red blood cell count, hemoglobin

concentration, and platelet count. Blood biochemical parameters, including liver function (eg, alanine aminotransferase, aspartate aminotransferase), renal function (eg, creatinine, urea nitrogen), lipid profile (eg, total cholesterol, triglycerides, high-density lipoprotein cholesterol, low-density lipoprotein cholesterol), and fasting blood glucose, were measured using an automated clinical chemistry analyzer (Cobas 8000 c702 module, Roche, Switzerland).Urinalysis was conducted with an automated urine sediment analysis system (UC-3500, Sysmex, Japan), which incorporates both dry chemistry reagent strips and automated sediment microscopy. Serum 25-hydroxyvitamin D [25-(OH)D] concentration was quantified by an electrochemiluminescence immunoassay on an automated immunoassay analyzer (Cobas e602 module, Roche, Switzerland).

Single-Cell Data Analysis

In this study, in order to deeply analyse the immune microenvironmental changes in adult males with different BMI status in the plateau hypoxic environment, we analysed the peripheral blood data of the volunteers after hypoxic stress by peripheral blood single-cell sequencing: all the volunteers collected peripheral blood samples by venepuncture on the 5th day of the plateau environment (Mardo County, Qinghai, China, altitude of 4200 m). Prior to sample collection, all volunteers signed an informed consent form and ethics committee approval was obtained.

The collected blood samples were immediately processed for isolation of single nucleated cells (PBMCs) using density gradient centrifugation to minimise contamination of erythrocytes and platelets. The isolated single nucleated cells were washed and resuspended, and adjusted to the appropriate cell concentration to ensure the quality and efficiency of subsequent single-cell sequencing.

In the analysis of single-cell transcriptomic data, we implemented stringent cell filtering criteria: cells were retained only if they met the following thresholds—detected genes between 200 and 8,000, total UMI counts below 50,000, and mitochondrial gene percentage less than 25%. Dimensionality reduction was performed using principal component analysis (PCA) in Seurat, and significant principal components (determined by JackStraw test, $p < 0.05$) were selected for subsequent clustering and UMAP visualization. Differential gene expression analysis was conducted using the Wilcoxon rank-sum test with thresholds set at $|\log_2 FC| \geq 0.36$, Bonferroni-adjusted p-value ≤ 0.01, and expression in more than 25% of cells within the target subpopulation. Bioinformatic analysis was performed using Omicsmart, a real-time interactive online platform for data analysis (http://www.omicsmart.com).[21–23]

Animal Experiment Validation (Key Biomarker and Immune Cell Subpopulation Validation)

Based on the results of the above single-cell data analysis and the validation of the screened key cell subpopulations and biomarkers, we selected 40 male SD rats (6-week-old SPF grade male SD rats (purchased from the Laboratory Animal Center of Beijing Weitong Lihua Experimental Animal Technology Co.) with an initial weight of 180 ~ 200 g), which were raised to adulthood with no restriction on diet and water before entering the plateau hypoxic stress, and then placed in a simulated low-pressure oxygen chamber at an altitude of 6000 m for 72 h to construct a hypoxic injury model, and collected peripheral blood tissues from the above rats and stored them in liquid nitrogen.[19] The peripheral blood tissues of the above rats were collected and stored in liquid nitrogen (For all animal experiments, the sample size per group was set at $n \geq 6$, based on established empirical laboratory practice).

After undergoing uniform acute hypoxic exposure, all rats were grouped based on the levels of biochemical markers reflecting tissue injury and inflammation (such as IFN-γ and TNF-α) in their peripheral blood. The 27 rats with the highest injury indicators were assigned to the severe injury group, while the 13 rats with the lowest indicators were assigned to the mild injury group. Subsequently, key biomarkers and cell subpopulations in the peripheral blood of these two groups were validated using flow cytometry and ELISA to determine their effectiveness in predicting the degree of hypoxic injury in animal experiments.

Flow Cytometry

This study utilized flow cytometry to detect regulatory T cells (Tregs) following a specific protocol. First, 200–500 μL of blood was collected from the abdominal aorta of SD rats using heparinized blood collection tubes (VHS02P, Weihai Saiwei Medical Technology Co., Ltd., China). Next, 3–5 times the volume of erythrocyte lysis buffer (number: 00-4300-

54, Thermo Fisher Scientific China) was added, and the mixture was gently vortexed and incubated at room temperature for 10–15 minutes, with gentle mixing twice during this period. The samples were then centrifuged at 4°C for 5 minutes at 450g, and the supernatant was discarded. The cell pellet was resuspended in 1 mL of PBS (#9808, Cell Signaling Technology, USA), centrifuged again, and the supernatant was discarded. Following this, 1 μL of CD25 antibody (MA5-17677, Thermo Fisher Scientific China) was added, and the mixture was incubated in the dark for 20 minutes. Afterward, 1 mL of 80% methanol (041467.K7, Thermo Fisher Scientific China) was added, mixed gently, and incubated for 5 minutes before centrifugation and discarding the supernatant. The cells were then treated with 1 mL of 0.1% PBS-Tween (PBS:79378, Tween:93773, Merck KGaA, Darmstadt, Germany), mixed, and incubated for 20 minutes, followed by another centrifugation and supernatant removal. Finally, 1 μL of FoxP3 antibody (12-5773-82, Thermo Fisher Scientific China) was added, and the cells were incubated in the dark for 20 minutes before being resuspended in PBS or flow cytometry buffer (PBS:79378, Merck KGaA, Darmstadt, Germany). The samples were then analyzed using a flow cytometer. To ensure the accuracy of the results, all antibodies used were validated, and appropriate controls were included.

ELISA

The Superoxide Dismutase (SOD), Glutathione Peroxidase (GSH-Px), Malondialdehyde (MDA), Hypoxia-Inducible Factor 1-α (HIF-1α), Interferon-γ (IFN-γ) and tumour necrosis factor α (TNF-α) content of the lung tissues were determined by using ELISA kits. The ELISA kits for SOD (ml077379), GSH-Px (ml107105), MDA (ml094971), HIF-1α (ml106668), IFN-γ (ml064291) and TNF-α (ml002859) were purchased from Shanghai Enzyme-linked Biological Co. Rat right upper lung tissues were weighed and put into a grinder for homogenization, and the supernatant was collected by centrifugation at a low temperature for 10 min. Above indexes were determined by using the ELISA kit, and the standard curve wells and detection wells were established. The optical density was measured at 450 nm using an ELISA kit, and the concentration of SOD, GSH-Px, MDA, HIF-1α, IFN-γ and TNF-α were calculated using a standard curve.

Strategy for Minimise Potential Confounders

Several strategies were implemented to minimise confounding: the order of treatments and measurements was randomised, investigators were blinded to group allocation during data collection and analysis, and cages from all groups were evenly distributed across racks and shelves to mitigate location bias; however, regular cage rotation was intentionally avoided to prevent stress-induced welfare confounders, though unmeasured location-specific factors may remain. Throughout the experiment, only the experimental operators were unblinded during the intervention due to the surgical nature; all other phases—including outcome assessment, and data analysis—were performed by personnel blinded to group allocation, with randomization sequences pre-generated and concealed until analysis completion.

Animal Care and Monitoring

Interventions to Reduce Pain, Suffering and Distress

To minimize animal pain and distress, all organism collection and experimental operation were performed under deep anesthesia using (sodium pentobarbital). For blood collection and injections, animals were briefly restrained using appropriate devices without anesthesia, and the use of atraumatic needles was ensured. All animals were housed in an enriched environment to reduce stress-related behaviors. Efforts were made to minimize the number of animals used and the duration of any potential suffering.

Expected or Unexpected Adverse Events

Adverse events were monitored throughout the study. As expected, the HFD group and hypoxia group exhibited signs of discomfort, including hair shedding and reduced activity, during the late stages of disease progression. No unexpected adverse events, such as unanticipated morbidity, self-mutilation, or severe infections, were observed in any of the control groups during the study period.

Humane Endpoints

Strict humane endpoints were established a priori and were prioritized over experimental endpoints. Animals were monitored at least twice daily, with increased frequency to every 4–6 hours for animals showing signs of progression. Endpoints included: (1) a weight loss exceeding 20% of initial body weight; (2) severe lethargy or an inability to access food or water; (3) the presence of ulcerated or necrotic tumors exceeding 1.5 cm in any diameter; (4) signs of severe pain or distress (prolonged hunched posture, vocalization). Any animal reaching any predefined humane endpoint was immediately humanely euthanized via (CO_2 inhalation followed by cervical dislocation) to prevent further suffering.

Statistical Analysis

The baseline data and LAKE LOUISE scores of the study data were statistically counted and analysed using SPSS 28.0 software, and the normality and variance chi-square of the data were tested using Kolmogoroe-Simirnov and Levene, respectively. Comparisons of data before and after the experiment in the same group were made using paired t-tests, and comparisons between two groups were made using independent samples t-tests. Statistical analysis of the remaining experimental results was performed using GraphPad Prism 10.4.0 software, data normality and homogeneity of variance were tested through Shapiro–Wilk tests and Levene's tests, respectively. When data exhibited normal distribution and homogeneity, independent samples t-tests (one-tailed) were employed for inter-group comparisons, while paired t-tests (one-tailed) were used for intra-group comparisons. For non-normal distributions or heteroskedastic conditions, the Mann–Whitney *U*-test was applied between groups, with Wilcoxon signed-rank tests implemented for intra-group comparisons. Related single-cell data analysis using were performed using R language and relevant statistical software. Appropriate statistical methods (*t*-test and ANOVA) were used to assess the differences in immune cell subpopulations at different time points and in different BMI states.All experimental results are expressed as mean ± standard deviation (Mean ± SD), $p < 0.05$ indicates significant differences, $p < 0.01$ indicates highly significant differences. GraphPad Prim10.4.0 and OriginPro2025 were used for drawing.

Results

Obese Rats Develop More Severe Hypoxic Injury

The body weight and Lee's index of rats in the normal chow group (NC) and high-fat chow group (HFD) increased with feeding time, and were significantly higher in the HFD group than in the NC group from the fourth week of feeding ($P < 0.05$) (Figure 1A and B). The total cholesterol, triglyceride and LDL levels in the blood of rats in the HFD group were significantly higher ($P < 0.0001$) (Figure 1C–E) and HDL levels were significantly lower ($P < 0.0001$) (Figure 1F) compared with those of rats in the NC group. In addition, the serum leptin content of rats in the HFD group was significantly higher than that of the NC group, and the serum lipocalin content showed the opposite trend of leptin change, which was significantly lower in the HFD group than in the NC group (Figure 1G and H). The above results suggest that an obese rat model can be successfully constructed by feeding rats with high-fat diet for 8 weeks (Figure 1).

Compared with the Control group, the partial pressure of oxygen and oxygen saturation of rats in the Obesity group decreased significantly ($P < 0.05$, $P < 0.01$) (Figure 2A and B). The H&E staining results of the lung tissue sections of rats in both groups showed that under the light microscope, the lung tissue of rats in the Control group was damaged in morphology and structure, with incomplete alveolar lumen structure, widened alveolar septum and infiltration of some erythrocytes and inflammatory cells (Figure 2C); the lung tissue of rats in the Obesity group had severe edema, with the lung tissue structure severely damaged, the alveolar septum widened significantly, and a large number of erythrocytes and inflammatory cells overflowed, and the degree of damage was greater than that of the Control group (Figure 2C). The level of oxidative stress in the lung tissues of rats in the Obesity group was significantly lower in SOD activity and GSH-Px content ($P<0.05$) (Figure 2E and F) and higher in MDA concentration ($P<0.05$) (Figure 2D) compared with that of the Control group, as shown by ELISA results (Figure 2). The above results suggest that obese rats are more susceptible to hypoxic stress in a hypoxic environment, leading to more severe hypoxic injury.

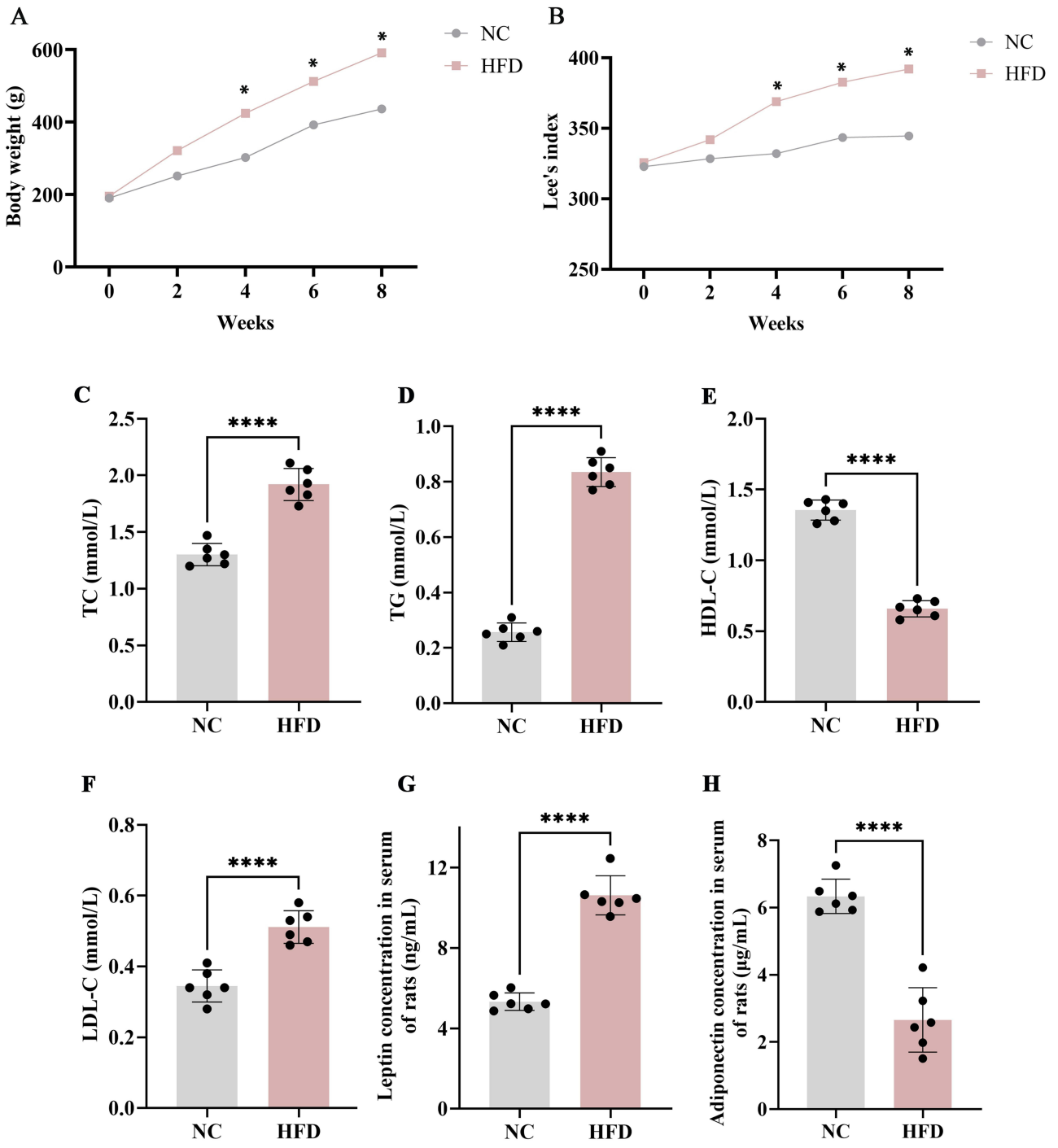

Figure 1 Construction of obese SD rat model. Using normal feed and high-fat feed to feed SD rats respectively for 8 weeks during the process of (**A**) changes in body weight and (**B**) changes in Lee's index; at the end of feeding ELISA to detect (**C**) serum total cholesterol content, (**D**) serum triglyceride content, (**E**) serum high-density lipoprotein (HDL) content, (**F**) serum low-density lipoprotein (LDL) content, (**G**) serum leptin content and (**H**) serum lipocalin content. *P < 0.05, ****P < 0.0001, n=6. Lee's index = {[body weight (g)]1/3/nasal-anal length (cm)}.

Abbreviations: NC, rats in normal chow-fed group; HFD, rats in high-fat chow-fed group.

Characteristics of the Participant and Clinical Data Analysis

Through voluntary recruitment, eight healthy, no underlying disease and previously living in the plains for a long period of time, with the no experience of travelling to high-altitude area activities, were included in this study. Table 1 We classified the above eight healthy young volunteers into normal group and obese group according to the level of BMI value, except for BMI, there was no significant difference in the baseline data of the above included study individuals.

https://doi.org/10.2147/JIR.S562386

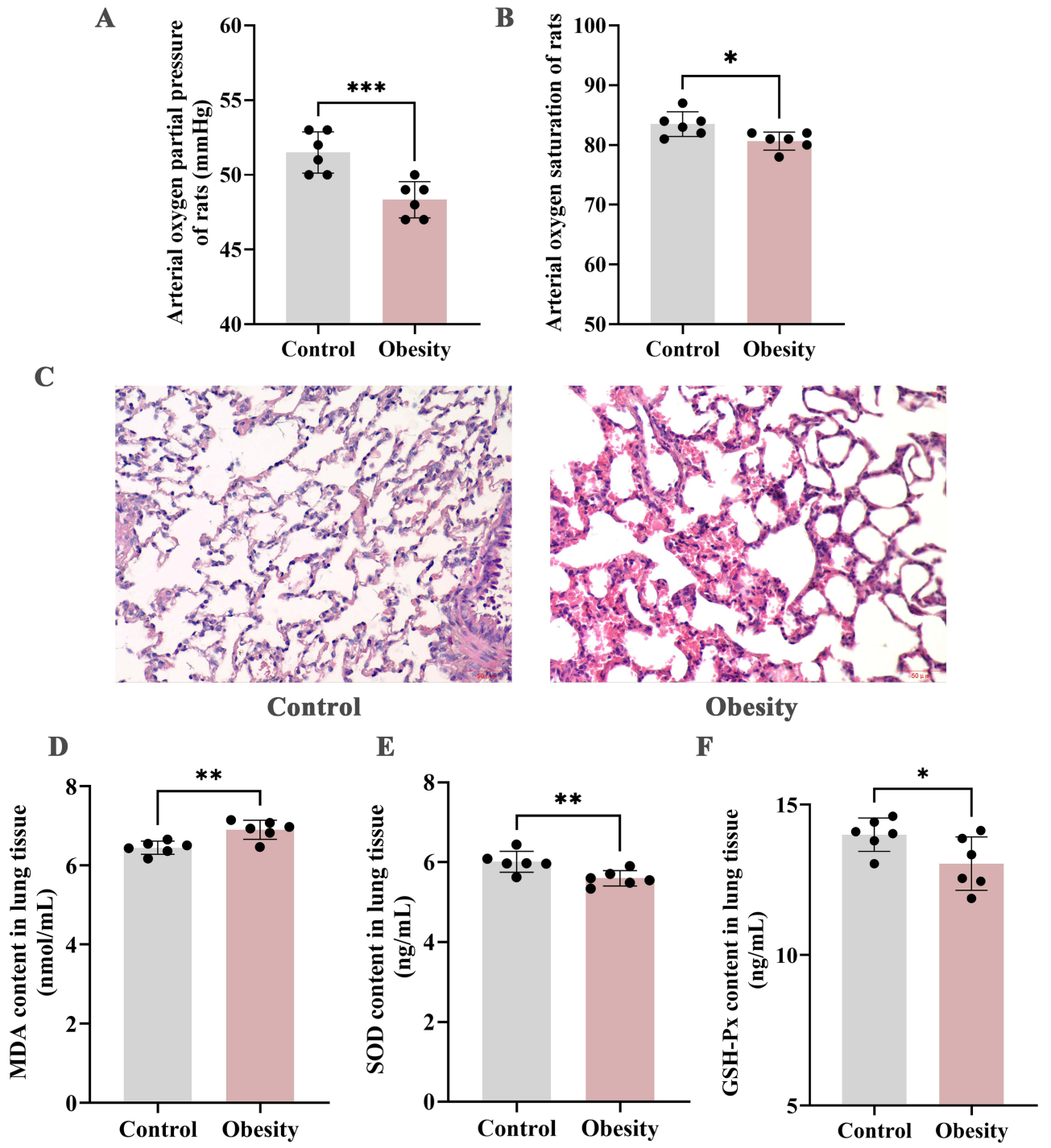

Figure 2 Effects of hypoxic stress on normal and obese rats. (**A**) Arterial blood oxygen partial pressure in rats, (**B**) blood oxygen saturation in rats, (**C**) H&E staining (400X) to observe the morphological changes in rat lung tissues, and (**D–F**) ELISA to detect the changes in oxidative stress levels in rat lung tissues. Control: normal rats under hypoxic stress conditions; Obesity: obese rats under hypoxic stress. Compared with Control group, *P < 0.05, **P < 0.01, ***P < 0.001, n=6.
Abbreviations: MDA, malondialdehyde; SOD, superoxide dismutase; GSH-Px, glutathione peroxidase.

We chose subjective and objective relevant clinical data as indicators to assess the plateau reaction situation of the two groups of patients, and we found that the patients in the obese group were consistent with the previous study, and all the indicators reflected a more serious plateau reaction state: among them, LLS and the vital signs indicators of the volunteers (Table 2) suggested that the obese population had a more serious plateau reaction state, and the clinical indicators (Figure 3A) also suggested a more severe inflammatory response in the obese population.

Table 1 Characteristics of the Participants in the Study

Variables	Normal (n=4)	Obesity (n=4)
Body mass index (kg/m^2)	21.34 ±2.44**	28.04 ± 0.48
Age (years)	23.5± 1.12	27.3 ± 1.92
Heart rate	71 ± 3.18	79 ± 3.89
Systolic blood pressure (mmHg)	110 ± 3.22	122± 4.29
Diastolic blood pressure (mmHg)	72 ± 3.22	69 ± 4.09
Pulse blood oxygen Saturation (%)	98 ± 0.83	98 ± 0.83
Underlying disease	No	No

Note: ***P < 0.01*.

Table 2 Characteristics of the Participants Under Hypoxia Stress for 5 Days

Variables	Normal (n=4)	Obesity (n=4)
Lake Louise Score ≥3	50% (n=2)	100% (n=4)
Headache example	50% (n=2)	100% (n=4)
Heart rate	96 ± 1.22	109 ± 3.11*
Systolic blood pressure (mmHg)	120 ± 4.24	137 ± 7.26*
Diastolic blood pressure (mmHg)	88.40 ± 5.26	93 ± 4.17
Pulse blood oxygen Saturation (%)	93 ± 2.11	90 ± 4.55*

Note: **P < 0.05*.

In previous studies, 25-(OH)D has been shown to inhibit inflammation and apoptosis to prevent and control the occurrence of altitude sickness, and 25-(OH)D was significantly lower in the obese group than in the normal group (Figure 3B), and based on our previous research data, it is suggested that this may be related to the severity of hypoxia injury.

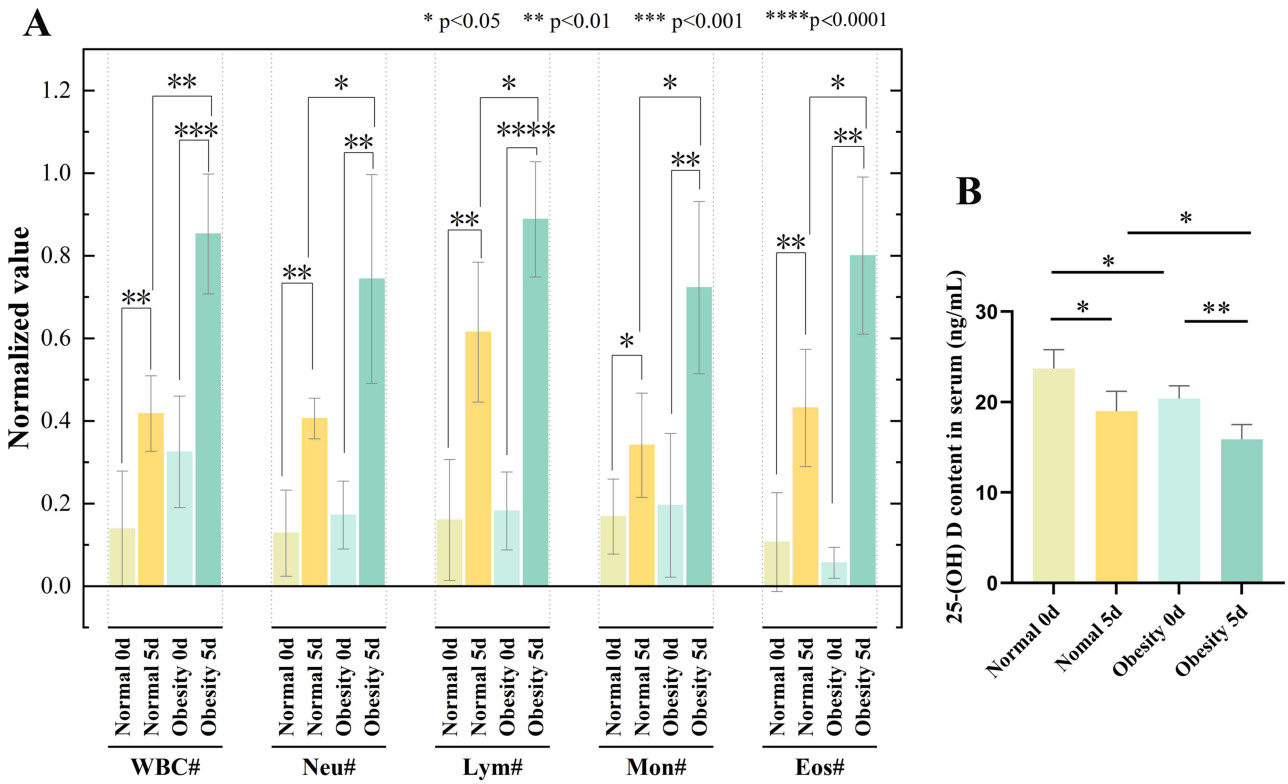

Figure 3 Clinical indicators of the participants under hypoxia stress for 5 days. (**A**) Clinical indicators of the participants under hypoxia stress, (**B**) 25-(OH)D of the participants under hypoxia stress. *P < 0.05, **P < 0.01, ***P < 0.001, ****P < 0.001.

https://doi.org/10.2147/JIR.S562386

Single-Cell Data Analysis

We integrated peripheral blood samples from 8 patients and successfully obtained a high-quality transcriptome of 36,949 single T cells. Unified Mobility Approximation and Projection (UMAP) analyses of these cells defined major T cells (Figure 4A–C).[24,25] And by comparatively analysing the differences in single cells between the two groups of volunteers, we found that the number of Treg cells in the obese group population was significantly lower than that in the normal body weight group population after hypoxic stress. Its key regulatory factor HIF-1α was significantly elevated under hypoxia, which further inhibited Treg cell activity, and the expression of Th17-related signaling pathway, NF-kappa B signaling pathway and HIF-1 signaling pathway were significantly elevated (Figure 4D and E).

Meanwhile, under hypoxic stimulation, the obese population showed stronger Tregs exhibiting altered fatty acid metabolism and mitochondrial adaptation, and increased production of IFN-γ and TNF-α, all of which coincided with the previous aggravation of hypoxic injury (Figure 4E).

Treg Cell Sub-Populations Can Serve as Hypoxic Injury Biomarker

There are differences in the number and function of Treg cells between obese and normal weight people after hypoxia stress, which may be a potential biomarker. In order to further explore the effectiveness of Treg cells as a biomarker for hypoxic injury, We carried out further validation in animals, and we found that by not restricting dietary water in rats after hypoxic stimulation could be divided into two groups according to the severity of their hypoxic response: severe injury group (> 6) and mild injury group (≤ 6) (Figure 5A), and the above grouping was mainly based on the hypoxic injury-related indexes and clinical manifestations in the pre-published data (Table 3).

Compared to the mild injury group, the severe injury group exhibited more significant lung tissue damage, characterized by markedly thickened alveolar septa and the infiltration of red blood cells and inflammatory cells into the alveolar spaces (Figure 5B). We compared the Treg cells and key transcription factors FOXP3, HIF-1α, IFN-γ and TNF-α in the above two groups of rats (Figure 5C–G), and we found that the number of Treg cells in the severely injured group was significantly lower than that in the mildly injured group, and the two groups of rats showed different trends of changes in Treg cells compared with the control group, and the key transcription factors also showed consistent trends with the single-cell data showed a consistent trend (Figure 5).

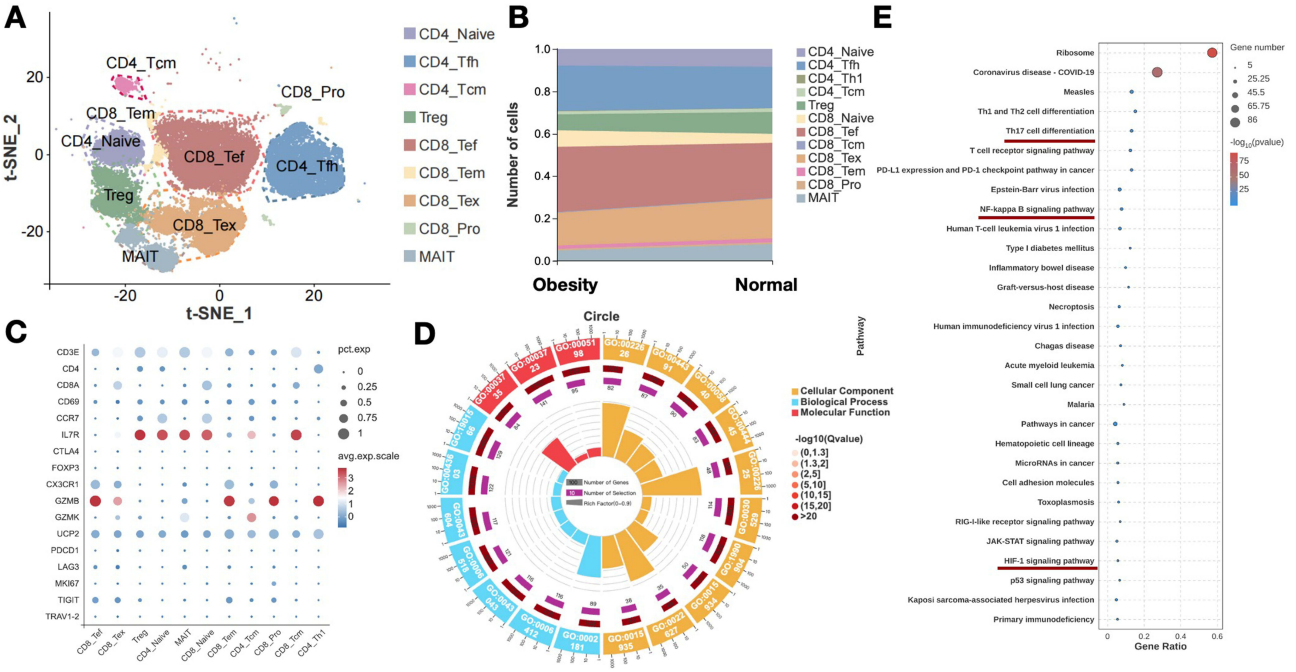

Figure 4 Single cell data of normal and obesity groups after hypoxia stress note. (**A**) UMAP analyses of major T cells; (**B**) The number of T cell subsets in different groups; (**C**) Key methods for defining T cell subsets; (**D** and **E**) Key Enrichment pathway in obese population.

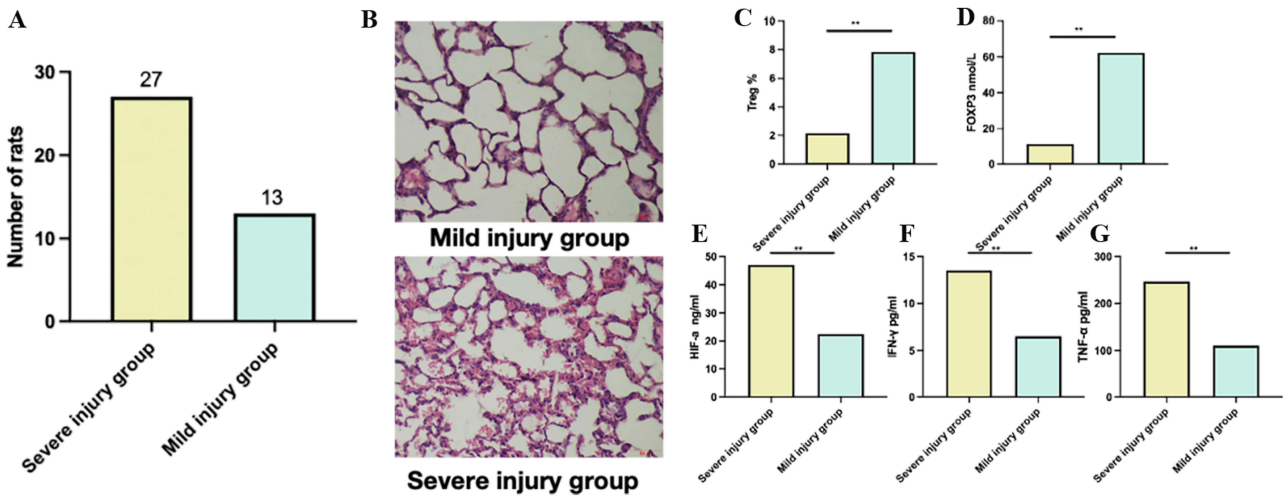

Figure 5 Treg Cell Subpopulations Can Serve as Hypoxic Injury Biomarker. (**A**) Final grouping based on the severity of hypoxia response in rats; (**B**) H&E staining (400X) to observe the morphological changes of lung tissue in severe injury group and mild injury group; (**C**) Changes in Treg cells of two groups of rats; (**D–G**) Changes in key transcription factors FOXP3, HIF-1α, IFN-γ, and TNF -α in two groups of rats.***P* < *0.01*.

Discussion

Rapid ascent to high altitude poses significant health risks, as acute hypoxic exposure can trigger a spectrum of clinical manifestations ranging from mild discomfort to life-threatening conditions such as high-altitude pulmonary edema and cerebral edema.[26] A key challenge in preventive medicine is identifying susceptible individuals prior to exposure. Our findings establish obesity as a critical predisposing factor for developing severe high-altitude illness. This conclusion is supported by converging evidence from controlled animal models and clinical observations. In animal models, obese rats exhibited exacerbated lung injury following hypoxia; in clinical observations, obese volunteers presented significantly more severe clinical responses. This heightened susceptibility aligns with the established understanding that obesity's inherent chronic low-grade inflammatory and metabolically dysregulated state creates a compromised baseline physiological condition.[27,28] When superimposed with the additional stress of hypoxia, this pre-existing condition appears to predispose individuals to a disproportionately severe inflammatory response.

To preliminarily investigate the underlying mechanisms, our single-cell RNA sequencing data revealed profound dysregulation of the immune landscape in obese individuals under hypoxic stress. The most prominent alteration was a marked reduction in circulating regulatory T cells (Tregs). Tregs are indispensable for maintaining immune tolerance and preventing excessive inflammation, a function particularly critical under physiological stress. While previous studies have established that hypoxia can disrupt Treg stability,[29–34] our data suggest the obese microenvironment amplifies this detrimental effect. We propose a mechanistic model wherein hypoxia-induced upregulation of HIF-1α plays a central role. Beyond its metabolic functions, HIF-1α is a potent immune modulator; its accumulation under low oxygen tension likely suppresses Treg activity and promotes their shift toward a pro-inflammatory Th17-like phenotype.[35–38] This phenotypic shift fundamentally skews the immune balance from a state of tolerance toward heightened inflammation, providing a plausible explanation for the exacerbated clinical manifestations.

Table 3 Hypoxic Injury Severity Scoring System

Variables	Value
Clinical signs of the organism (death, cyanosis, mobility, etc.)	2
PaO_2 < 60mmHg or SaO_2 < 85%	2
Significant damage to lung tissue sections (oedema, inflammatory exudates, etc.)	2
Inflammatory Storms	2
Elevated apoptosis, damage indicators	2

https://doi.org/10.2147/JIR.S562386

Furthermore, our data indicate that Tregs from obese individuals under hypoxia exhibit distinct metabolic alterations and increased production of IFN-γ and TNF-α.[39–41] We hypothesize that pre-existing metabolic dysregulation in obesity predisposes Tregs to functional failure upon encountering the "second hit" of hypoxic stress. The consequent loss of immunosuppressive capacity and acquisition of pro-inflammatory properties directly contribute to the aggravated injury.

To translate this mechanistic insight into a practical tool, we validated the value of Tregs as a biomarker in animal models. Establishing and successfully validating injury severity thresholds based on Treg levels and related inflammatory cytokines (IFN-γ, TNF-α) moves beyond mere association.[42,43] It provides a quantitative framework that positions Tregs and their downstream effectors as components of a predictive immunological signature for assessing individual risk upon acute high-altitude ascent.

This study proposes a novel evaluative biomarker for severe high-altitude reactions in acutely exposed populations. However, several limitations should be acknowledged. The clinical sample size was limited, and the validation of Tregs as a biomarker was conducted only in animal experiments, warranting further investigation in human cohorts. Due to experimental constraints, the number of included obese and normal-weight participants was relatively small, and we plan to expand this cohort in future studies. Additionally, the animal validation experiments employed an established hypoxic injury model rather than identical hypoxic stress conditions used elsewhere. The lack of correlation analysis with key hematological indicators (eg, hemoglobin concentration) limits a comprehensive understanding of the physiological mechanisms of high-altitude adaptation. To address this, subsequent research will systematically integrate immunological data with hematological and physiological parameters to construct a more comprehensive pathophysiological model of high-altitude illness. We will continue to explore the feasibility of Tregs as biomarkers under different conditions, particularly in field studies of hypoxic injury at various altitudes.

Furthermore, the core pathophysiology of high-altitude illnesses resides in tissue-specific microenvironments, such as the local inflammatory infiltration in pulmonary vascular beds during the development of high-altitude pulmonary hypertension, and the chronic inflammatory state of adipose tissue which functions as a major endocrine and immune organ in obese individuals. Our study did not perform lineage analysis of tissue-resident immune cells in bronchoalveolar lavage fluid (BALF) or adipose tissue, nor did we provide broader cytokine multiplex detection data, suggesting potential oversight of key local immune events driving disease progression. Notably, the inherent adipose tissue inflammation in obese individuals may become amplified under acute hypoxic stress and systematically influence circulating immune cell function through specific inflammatory mediators (eg, leptin, IL-6). This potential confounding effect remains incompletely resolved by our current data. Consequently, future studies should essentially integrate circulating immune parameters with tissue-specific immune profiles (eg, via bronchoalveolar lavage or adipose tissue biopsies). Our current work, by revealing the distinct peripheral immune signature in obesity under acute hypoxia, establishes a solid foundation and provides clear direction for these crucial subsequent investigations—specifically focusing on the interplay between immunoregulatory pathways (including Treg cells) in both tissue-localized and systemic circulation.

Limitations and Future Directions

This study has several limitations that warrant consideration. First, the relatively small sample size of population cohort may limit the statistical power. Second, although our analysis suggests that Treg cells could serve as a biomarker for hypoxic injury, this phenotypic observation still lacks validation in human studies. Furthermore, the comparison between normoxic and hypoxic conditions in normal-weight versus obese populations, as well as the underlying mechanisms driving changes in the immune microenvironment, were not deeply explored. Importantly, we did not assess the dynamic changes of these parameters in population subjects. We will continue to expand this part of the study to explore the feasibility of Treg cells as biomarkers under different conditions, especially under different poster heights of hypoxic injury in the field, in order to lay the foundation for its further application in the clinic.

Conclusion

In this study, we initially mapped the single-cell profile of acute hypoxic injury in obese population and found that the number of Treg cell subpopulation is lower in obese population who rush into plateau, which may be related to the fact that this kind of patients have more severe hypoxic response, and initially verified its validity as a Biomarker in animals, which lays the

foundation for its development into a biomarker that may predict the severity of the onset of plateau response. It lays the foundation for its development as a possible biomarker for predicting the severity of the onset of altitude sickness.

Abbreviations

SPF, Specific Pathogen Free; AMS, Altitude Mountain Sickness; TC, Total cholesterol; TG, triglycerides; LDL, low-density lipoprotein; HDL, high-density lipoprotein; VLDL, very-low-density lipoprotein; LLS, Lake Louise Score; SOD, Superoxide Dismutase; GSH-Px, Glutathione Peroxidase; MDA, Malondialdehyde; HIF-1α, Hypoxia-Inducible Factor 1-α; IFN-γ, Interferon-γ; TNF-α, tumour necrosis factor α; UMAP, Unified Mobility Approximation and Projection.

Data Sharing Statement

The data that support the findings of this study are not openly available due to sensitivity and volunteer privacy, but they are available from the corresponding author upon reasonable request.

Ethics Declarations

Human Ethics and Consent to Participate declarations: This research has passed the ethical review of medical science research by the Medical College of Qinghai University (Approved on July 24, 2020), and has been approved by the Ministry of Science and Technology of the People's Republic of China to collect Chinese human genetic resources. The batch number is: [2024]CJ0016, allow the collection of human samples. All volunteers are aware of the experimental content and voluntarily participate. In case of emergencies, all volunteers have the right to choose to withdraw from the experiment, the work described has been carried out in accordance with The Code of Ethics of the World Medical Association (Declaration of Helsinki) for experiments involving humans. Animal Ethics: The animal handling measures involved in the implementation of this project are carried out in accordance with the national "Guidelines for Ethical Review of Experimental Animal Welfare" (GB/T35892-2018) and have been approved by Science and Technology Ethics Committee of Qinghai University (Approved on July 24, 2020). The animal experiments involved in this study were conducted in accordance with the ARRIVE guidelines.

Acknowledgments

Thanks to the Omicsmart platform. Bioinformatic analysis was performed using Omicsmart, a real-time interactive online platform for data analysis (http://www.omicsmart.com).

Author Contributions

Xiaoyan Pu: Conceptualization, Funding acquisition, Data curation, Formal analysis, Investigation, Project administration, Methodology, Validation, Visualization, Writing-review and editing. Yaxuan Wang: Conceptualization, Data curation, Formal analysis, Investigation Methodology, Validation, Visualization, Writing-original draft. Xue Lin: Conceptualization, Data curation, Formal analysis, Investigation Methodology, Validation, Visualization, Writing-original draft. Jun Zhao: Investigation, Validation, Visualization, Writing-review and editing. Chongyang Dai: Investigation, Validation, Visualization, Writing-original draft. Yonggui Ma: Conceptualization, Funding acquisition, Investigation, Methodology, Project administration, Resources and Supervision, Writing-review and editing. Peijun Shi: Conceptualization, Funding acquisition, Investigation, Methodology, Project administration, Resources and Supervision, Writing-review and editing. All authors took part in drafting, revising or critically reviewing the article, gave final approval of the version to be published, have agreed on the journal to which the article has been submitted, and agree to be accountable for all aspects of the work.

Funding

This study was financially supported by the National Natural Science Foundation of China (82160322); The Second Comprehensive Scientific Expedition to the Qinghai Tibet Plateau (2019QZKK0606-02); Central guidance of local scientific and technological development funds in Qinghai Province (2025-ZY-044).

Disclosure

The authors have no competing interests in this paper.

References

1. Luks AM, Hackett PH. Medical conditions and high-altitude travel. *N Engl J Med*. 2022;386:364–373. doi:10.1056/NEJMra2104829
2. Ogilvie RI. High-altitude illness. *N Engl J Med*. 2001;345(17):1279–1280. doi:10.1056/NEJM200110253451713
3. Dunham-Snary KJ, Wu D, Sykes EA, et al. Hypoxic pulmonary vasoconstriction: from molecular mechanisms to medicine. *Chest*. 2016;151(1):181–192. doi:10.1016/j.chest.2016.09.001
4. Gatterer H, Villafuerte FC, Ulrich S, et al. Altitude illnesses. *Nat Rev Dis Primers*. 2024;10:1. doi:10.1038/s41572-024-00526-w
5. Wu TY, Ding SQ, Liu JL, et al. Who should not go high: chronic disease and work at altitude during construction of the Qinghai-Tibet railroad. *High Alt Med Biol*. 2007;8(2):88–107. doi:10.1089/ham.2007.1015
6. Bhattacharya S, Shrimali NM, Mohammad G, Koul PA, Prchal JT, Guchhait P. Gain-of-function Tibetan PHD2$^{D4E;C127S}$ variant suppresses monocyte function: a lesson in inflammatory response to inspired hypoxia. *EBioMedicine*. 2021;68:103418. doi:10.1016/j.ebiom.2021.103418
7. Li S, Xue G, Zhao H, et al. The mycoplasma pneumoniae HapE alters the cytokine profile and growth of human bronchial epithelial cells. *Biosci Rep*. 2019;39(1):BSR20182201. doi:10.1042/BSR20182201
8. Wu XH, Zhang Z, Zhang L, et al. Single-cell analysis of peripheral blood from high-altitude pulmonary hypertension patients identifies a distinct monocyte phenotype. *Nat Commun*. 2023;14(1):1820. doi:10.1038/s41467-023-37527-4
9. Deng X, Wang L, Zhai Y, et al. RIPK1 plays a crucial role in maintaining regulatory T-cell homeostasis by inhibiting both RIPK3- and FADD-mediated cell death. *Cell Mol Immunol*. 2024;21(1):80–90. doi:10.1038/s41423-023-01113-x
10. Feldhoff LM, Rueda CM, Moreno-Fernandez ME, et al. IL-1β induced HIF-1α inhibits the differentiation of human FOXP3^{+} T cells. *Sci Rep*. 2017;7:465. doi:10.1038/s41598-017-00508-x
11. Dixon JB. Obesity and diabetes: the impact of bariatric surgery on type-2 diabetes. *World J Surg*. 2009;33(10):2014–2021. doi:10.1007/s00268-009-0062-y
12. Trayhurn P. Hypoxia and adipose tissue function and dysfunction in obesity. *Physiol Rev*. 2013;93(1):1–21. doi:10.1152/physrev.00017.2012
13. Kayser B, Verges S. Hypoxia, energy balance, and obesity: an update. *Obes Rev*. 2021;22(Suppl 2):e13192. doi:10.1111/obr.13192
14. Siques P, Brito J, Ordenes S, et al. Involvement of overweight and lipid metabolism in the development of pulmonary hypertension under conditions of chronic intermittent hypoxia. *Pulm Circ*. 2020;10(S1):42–49. doi:10.1177/2045894020930626
15. Calcaterra V, Croce S, Vinci F, et al. Th17 and Treg balance in children with obesity and metabolically altered status. *Front Pediatr*. 2020;8:591012. doi:10.3389/fped.2020.591012
16. Matarese G. The link between obesity and autoimmunity. *Science*. 2023;379(6639):1298–1300. doi:10.1126/science.ade0113
17. Trinchese G, Cimmino F, Catapano A, et al. Mitochondria: the gatekeepers between metabolism and immunity. *Front Immunol*. 2024;15:1334006. doi:10.3389/fimmu.2024.1334006
18. Li Z, Zhang B, Wang N, et al. A novel peptide protects against diet-induced obesity by suppressing appetite and modulating the gut microbiota. *Gut*. 2023;72(4):686–698. doi:10.1136/gutjnl-2022-328035
19. Lin X, Lei YF, Pu XY. 不同低氧胁迫方式构建SD大鼠高原肺水肿模型的比较研究 [Comparative study on the construction of high altitude pulmonary edema models in SD rats by different hypoxia stress methods]. *Lab Anim Comp Med*. 2020;40(5):367–373. Chinese. doi:10.3969/j.issn.1674-5817.2020.05.002
20. Roach RC, Hackett PH, Oelz O, et al. The 2018 Lake Louise acute mountain sickness score. *High Alt Med Biol*. 2018;19(1):4–6. doi:10.1089/ham.2017.0164
21. McGinnis CS, Murrow LM, Gartner ZJ. DoubletFinder: doublet detection in single-cell RNA sequencing data using artificial nearest neighbors. *Cell Syst*. 2019;8(4):329–337. doi:10.1016/j.cels.2019.03.003
22. Chung NC, Storey JD. Statistical significance of variables driving systematic variation in high-dimensional data. *Bioinformatics*. 2015;31(4):545–554. doi:10.1093/bioinformatics/btu674
23. Camp JG, Sekine K, Gerber T, et al. Multilineage communication regulates human liver bud development from pluripotency. *Nature*. 2017;546(7659):533–538. doi:10.1038/nature22796
24. Zhang C, Li J, Cheng Y, et al. Single-cell RNA sequencing reveals intrahepatic and peripheral immune characteristics related to disease phases in HBV-infected patients. *Gut*. 2023;72(1):153–167. doi:10.1136/gutjnl-2021-325915
25. Liu Y, Zhang Q, Xing B, et al. Immune phenotypic linkage between colorectal cancer and liver metastasis. *Cancer Cell*. 2022;40(4):424–437. doi:10.1016/j.ccell.2022.02.013
26. Golden A. Obesity's impact. *Nurs Clin North Am*. 2021;56(4):xiii–xiv. doi:10.1016/j.cnur.2021.08.004
27. Frid MG, Brunetti JA, Burke DL, et al. Hypoxia-induced pulmonary vascular remodeling requires recruitment of circulating mesenchymal precursors of a monocyte/macrophage lineage. *Am J Pathol*. 2006;168(2):659–669. doi:10.2353/ajpath.2006.050599
28. Byon CH, Javed A, Dai Q, et al. Oxidative stress induces vascular calcification through modulation of the osteogenic transcription factor Runx2 by AKT signaling. *J Biol Chem*. 2008;283(22):15319–15327. doi:10.1074/jbc.M800021200
29. Kang JH, Zappasodi R. Modulating Treg stability to improve cancer immunotherapy. *Trends Cancer*. 2023;9(11):911–927. doi:10.1016/j.trecan.2023.07.015
30. Yano H, Andrews LP, Workman CJ, et al. Intratumoral regulatory T cells: markers, subsets and their impact on anti-tumor immunity. *Immunology*. 2019;157(3):232–247. doi:10.1111/imm.13067
31. Wang H, Franco F, Ho PC. Metabolic regulation of Tregs in cancer: opportunities for immunotherapy. *Trends Cancer*. 2017;3(8):583–592. doi:10.1016/j.trecan.2017.06.005
32. Zhang C, Qiao Y, Huang L, et al. Regulatory T cells were recruited by CCL3 to promote cryo-injured muscle repair. *Immunol Lett*. 2018;204:29–37. doi:10.1016/j.imlet.2018.10.004
33. Zhang C, Li L, Feng K, et al. 'Repair' Treg cells in tissue injury. *Cell Physiol Biochem*. 2017;43(6):2155–2169. doi:10.1159/000484295

34. Loffredo LF, Savage TM, Ringham OR, et al. Treg-tissue cell interactions in repair and regeneration. *J Exp Med*. 2024;221(6):e20231244. doi:10.1084/jem.20231244
35. Sivasami P, Elkins C, Diaz-Saldana PP, et al. Obesity-induced dysregulation of skin-resident PPARγ+ Treg cells promotes IL-17A-mediated psoriatic inflammation. *Immunity*. 2023;56(8):1844–1861. doi:10.1016/j.immuni.2023.06.021
36. Becker M, Joseph SS, Garcia-Carrizo F, et al. Regulatory T cells require IL6 receptor alpha signaling to control skeletal muscle function and regeneration. *Cell Metab*. 2023;35(10):1736–1751. doi:10.1016/j.cmet.2023.08.010
37. Li C, Wang G, Sivasami P, et al. Interferon-α-producing plasmacytoid dendritic cells drive the loss of adipose tissue regulatory T cells during obesity. *Cell Metab*. 2021;33(8):1610–1623. doi:10.1016/j.cmet.2021.06.007
38. Elkins C, Li C. Deciphering visceral adipose tissue regulatory T cells: key contributors to metabolic health. *Immunol Rev*. 2024;324(1):52–67. doi:10.1111/imr.13336
39. Soedono S, Sharlene S, Vo DHN, et al. Obese visceral adipose dendritic cells downregulate regulatory T cell development through IL-33. *Front Immunol*. 2024;15:1335651. doi:10.3389/fimmu.2024.1335651
40. Lao P, Chen J, Tang L, et al. Regulatory T cells in lung disease and transplantation. *Biosci Rep*. 2023;43(10):BSR20231331. doi:10.1042/BSR20231331
41. Zhang S, Gang X, Yang S, et al. The alterations in and the role of the Th17/Treg balance in metabolic diseases. *Front Immunol*. 2021;12:678355. doi:10.3389/fimmu.2021.678355
42. Dai C, Lin X, Wang YX, et al. 骨化三醇通过B细胞受体/PI3K/AKT/NF-κB通路抑制大鼠高原肺水肿的发生 [Calcitriol inhibits B-cell receptor/PI3K/AKT/NF-κB pathway to improve high altitude pulmonary edema in rats]. *Chin J Anat*. 2023;46(5):379–384. Chinese.
43. Dai C, Lin X, Qi Y, et al. Vitamin D3 improved hypoxia-induced lung injury by inhibiting the complement and coagulation cascade and autophagy pathway. *BMC Pulm Med*. 2024;24(1):9. doi:10.1186/s12890-023-02784-y